

# The Influence of Omni – Directional Guide Vane on the Cross – Flow Wind Turbine Performance

Yahya<sup>1</sup>, Fahrudin<sup>2</sup>, Budhi Martana<sup>3</sup>

(Received: 29 October 2024 / Revised: 05 November 2024 / Accepted: 15 November 2024 / Available Online: 31 December 2024)

**Abstract**—As cities grow, the demand for energy increases, necessitating a corresponding increase in energy supply. Since urban areas consume the majority of the world's energy, switching to renewable energy sources is essential. Wind energy is one of the most popular renewable energy sources for generating electricity. Vertical-axis wind turbines (VAWTs) are used in urban areas due to their advantages, with cross-flow wind turbines (CFWTs) being one type. However, the efficiency of CFWTs is relatively low, necessitating the application of augmentation devices. This study aims to find the optimal configuration between CFWTs and Omni-Directional Guide Vanes (ODGV), using 6DOF dynamic mesh methods in ANSYS Fluent with varying the turbine blade counts and the addition of ODGV. The results showed that the 18-blade configuration exhibits the highest improvement with ODGV, demonstrating a remarkable 71 percent increase in the power coefficient. In general, the highest performance is achieved by the 20-blade turbine with a 6-blade ODGV configuration, with a power coefficient of 0.2455, which is 30 percent higher than the baseline 20-blade turbine. These findings indicate that the addition of ODGV significantly improves the performance of cross-flow wind turbines.

**Keywords**—augmented devices, coefficient of power, cross-flow wind turbine, performance, urban areas.

## I. INTRODUCTION

Urban areas and cities play a major role in the sustainable energy transition. As a city grows, the demand for energy increases and the supply of energy must increase. Since cities consume the majority of the world's energy, switching to the use of renewable energy is essential [1]. Renewable energy was chosen as a solution to the energy crisis because it is abundant and can be utilized continuously without thinking about its side effects. Due to its abundance, affordability, and efficiency, wind energy is one among the most popular renewable energy sources for producing electricity [2]. One tool for converting wind energy is a wind turbine. Based on how they rotate, wind turbines are classified as either horizontal-axis (HAWT) or vertical-axis wind turbines (VAWT) [3]. VAWTs can be used in urban areas because they can pick up wind from any direction [4]. This wind turbine is more practical in urban areas because it can collect wind energy without requiring a large land area. This turbine can harvest wind energy despite wind turbulence generated by buildings in urban areas. In addition, VAWTs do not make too much noise and therefore do not cause noise pollution. Lastly, these wind turbines have a low cut-in speed so they can operate at low speeds, for example in urban areas [5]. Given these advantages, VAWTs are a promising technology when the demand for renewable energy is high.

The Cross-Flow Wind Turbine (CFWT), one of the various model variants for VAWT, has geometric similarities with the Savonius Wind Turbine [6]. Since this turbine is an adaptation of the Banki water turbine, the idea and operation of cross-flow wind turbines are similar to those of water turbines [7].

Several studies related to cross-flow wind turbines usually discuss performance optimization through parameter and configuration changes [8], [9], blade orientation and shape [10], and the addition of augmentation devices [11], [12], [13].

Since the efficiency of CFWTs is still relatively low and the available wind flow is unpredictable, an augmentation device to improve wind energy capture was created. One such device is the ODGV. ODGV (Omni-Directional Guide Vane) is a wind flow direction system used in CFWT with geometry in the form of static blades whose role is to direct the wind from all directions towards CFWT [14]. The efficiency of wind turbines can be greatly increased by combining ODGV with CFWT. ODGV can be used to optimized the wind flow direction prior to it reaching the turbine, as well as to improve the wind speed that will reach the turbine [15].

Several studies have been conducted to improve the performance of CFWT by applying augmentation devices. Wicaksono, Tjahjana and Hadi evaluated the impact of ODGV to the performance of CFWT where ODGV can enhance the efficiency of CFWT, particularly in areas with challenging wind conditions. Their research using wind tunnel experiments, which revealed that the

<sup>1</sup>Yahya is with Departement of Mechanical Engineering, Universitas Pembangunan Nasional Veteran Jakarta, Jakarta, 12450, Indonesia. E-mail: yahyanemos@gmail.com

<sup>2</sup>Fahrudin is with Departement of Mechanical Engineering, Universitas Pembangunan Nasional Veteran Jakarta, Jakarta, 12450, Indonesia. E-mail: fahrudin@upnvj.ac.id

<sup>3</sup>Budhi Martana is with Departement of Mechanical Engineering, Universitas Pembangunan Nasional Veteran Jakarta, Jakarta, 12450, Indonesia. E-mail: budhi.martana@upnvj.ac.id

maximum power coefficient is 0.125 at 60° wind direction, which is 21.46% greater than those without ODGV. This result concluded that the ODGV plays a crucial role to enhance the efficiency of CFWT in urban environment [13]. Further research by Wibowo, Tjahjana, Santoso and Situmorang has done the experimental test to assess various configurations of turbines and ODGV with focus on the number of blades and the tilt angles of the ODGV. From the experiment, the optimal configuration was found in the 60° ODGV tilt angle, with 16 ODGV blades and 16 turbine blades, with the power generated increasing by 271.39% compared to the configuration without using ODGV. The study concluded that configurations with more guide vanes blades than turbine blades can generate higher power outputs, provided the numbers are closely matched [12]. Another research is conducted by Yahya, et al. who examined different configurations of the CFWT, including variations in blade counts and guide vane setups, under multiple tilt angles and wind speeds. The research finding indicated that the optimal configuration is a turbine with 14-blade ODGV at a 55° angle had the maximum power coefficient, which is 0.0162 at a TSR of 0.289, where this value increased by about 59% compared to the turbine performance without using ODGV [16]. R. Iliev also conducted research with aims to enhance the performance of CFWT by using an

omni-directional multi-nozzle, an unique guiding device that utilizes the Venturi effect to optimize airflow dynamics around turbine runner. The research indicate that the omni-directional multi-nozzle is significantly enhance the performance of CFWT by nearly double the efficiency of the base turbine [11]. Other research by V. Obretenov and R. Iliev that aims to enhance the performance of CFWT with a frontal cylindrical guide vane unit. The result suggest that the cylindrical guide vane act more like deflectors rather than flow directors, ultimately improving the turbine's performance [17]. On the other hand, K. Kolodziejczyk and R. Ptak has conducted the study to enhance the performance of CFWT with curve-shaped ODGV. From the study, it concluded that the guide vanes significantly enhance the turbine's performance, especially in variable wind conditions. Maximum power coefficient achieved by their turbine is 22% at tip speed ratio of 0.7, which is a good value for a vertical-axis wind turbine [18].

This study focuses on the analysis of the performance of cross-flow wind turbines using method of Computational Fluid Dynamics by varying the number of turbine blades and adding Omni-Directional Guide Vane to improve its performance. This study aims to find the best configuration of wind turbine and ODGV.

TABLE 1.

CROSS-FLOW WIND TURBINE MODEL SPESIFICATION	
Spesification	Value
Diameter, D	200 mm
Blade Length, L	250 mm
Number of Blades, N	16, 18, 20
Pitch Angle	45
Chord Length	22 mm
Camber Line	Circular Arc
Camber Line Radius	20 mm
Maximum Airfoil Thickness	4 mm
Leading Edge Radius	1 mm

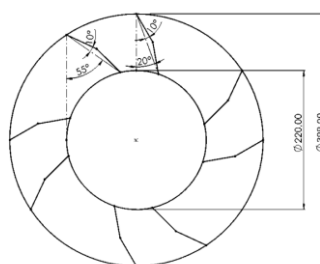


Figure 1. Guide Vane Model

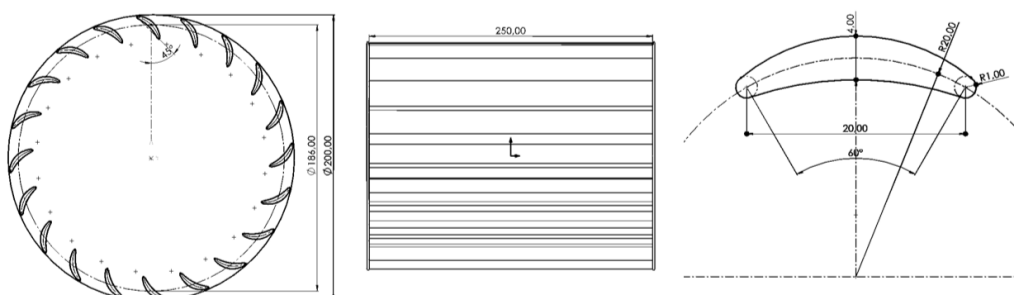


Figure 2. Cross-flow wind turbine model and airfoil

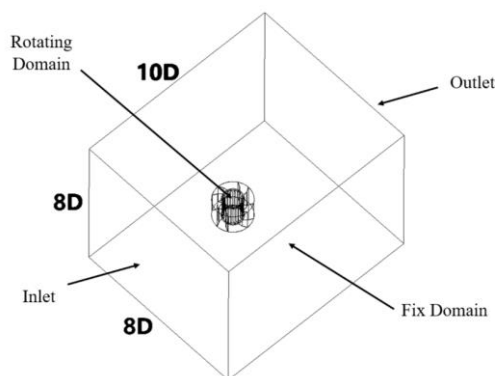


Figure 3. Computational Domain of Turbine and Guide Vane

TABLE 2.  
 INPUT PARAMETER FOR BOUNDARY CONDITIONS

Parameter	Description
Inlet	Velocity Inlet
Outlet	Pressure Outlet
Interface	No Condition
Wall	Non-Slip

## II. METHOD

### A. Turbine Models

The cross-flow wind turbine model used in the current study had geometry displayed in Figure 2. This model refers to the model designed by Tanino, et al. [19] with detailed specifications are represented in TABLE 1. The simulation of this model is carried out with varying the number of turbine blade, with 16, 18 and 20 blades.

### B. Guide Vane Models

Figure 1 shows the geometry of the ODGV used as a turbine performance enhancer. The ODGV model used in this study refers to research by Wong, et al. [20]. With tilt angle of 55° and 20° and variation in blade numbers of 6 and 8 blades.

### C. Computational Domain

This study's computational domain is depicted in Figure 3. The rectangular domain is the fixed domain and the cylinder domain is the rotating domain. The rotor is located inside the rotating domain, which is 4D from the wall and inlet. The domain size is 8D x 8D x 10D where D is the rotor diameter.

### D. Meshing

Figure 4 shows the mesh around turbine models. The

mesh around turbine blades and ODGV is finer and denser than the mesh that away from the blades. The mesh size in the rotating domain and the rotor respectively are 2 mm and 0.5 mm. This size is obtained after conducting a mesh independence test where in this test the mesh size and shape are varied to get the best mesh setup to obtain accurate results and not sacrifice a very long simulation time [21].

### E. Boundary Condition

The boundary conditions of the study can be seen in Figure 3. The rotor surface is set as a non-slip wall. The input parameters for the boundary conditions can be seen in TABLE 2. The inlet velocity is set at 3.4 m/s. The outlet pressure is set at atmospheric pressure.

### F. Numerical Method

ANSYS Fluent is used for the simulation in this study. The simulation was conducted in an unsteady state with the k- $\omega$  SST viscosity model. This model is used because it is the combination of k- $\omega$  model in near-wall region and standard k- $\epsilon$  in the region that far from the wall [22], [23]. The simulation in this study was carried out using the Dynamic Mesh 6 DOF method. This method was chosen because of its advantages that can show how the actual situation where the turbine is driven by the wind [24].

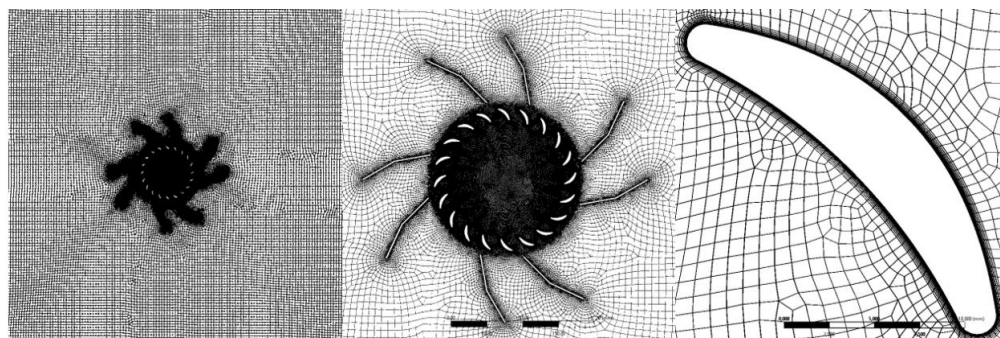


Figure 4. Mesh of the computational domain

TABLE 6.  
 MAXIMUM POWER COEFFICIENT FOR 20-BLADE CROSS-FLOW WIND TURBINE

Variation	Cp	Improvement (%)
Without ODGV	0.18888234	--
6-Blade ODGV	0.245503253	30%
8-Blade ODGV	0.208958788	11%

TABLE 6.  
 MAXIMUM POWER COEFFICIENT FOR 18-BLADE CROSS-FLOW WIND TURBINE

Variation	Cp	Improvement (%)
Without ODGV	0.127313172	--
6-Blade ODGV	0.217655286	71%
8-Blade ODGV	0.189732874	49%

TABLE 6.  
 MAXIMUM POWER COEFFICIENT FOR 16-BLADE CROSS-FLOW WIND TURBINE

Variation	Cp	Improvement (%)
Without ODGV	0.148739	--
6-Blade ODGV	0.180505	21%
8-Blade ODGV	0.189902	28%

TABLE 6.  
 DATA VALIDATIONS WITH PREVIOUS STUDY

Study	Coefficient of Power	Error
Tanino	0.1	-
Yahya	0.114	1.39%

G. Research Validation

The simulation results were validated with previous research to make the calculations match. This study was validated with research by Tanino, et al. [19] to determine the error value in this validation, the power coefficient (Cp) value is compared with that of the previous study. The validation results can be seen in TABLE 6.

III. RESULTS AND DISCUSSION

A. Power Coefficient

Figure 5 is the graph of the power coefficient generated by each turbine configuration obtained from the fluid flow simulations that have been carried out. This graph provides the difference of the performance of wind turbine under various configurations. The x-axis represents the different turbine configurations, while the y-axis is the corresponding power coefficient values.

Figure 5 shows that a wind turbine with an ODGV installed performs better than without an ODGV. This is shown by the higher power coefficient values. In the

graph, the data points show a clear upward trend for the configurations with ODGV, highlighting their efficiency. This shows that the influence of the ODGV can increase the power coefficient of the turbines. The highest power coefficient is obtained by configuration model 20B60 with power coefficient value of 0.2455.

The improvement of the power coefficient for each turbine blade change can be seen in TABLE 5 - TABLE 3. The improvement varies according to the number of ODGV blades and is compared with the base turbine without it.

For 16-blade turbine configurations, the performance improvement with the addition of an ODGV is clearly illustrated in TABLE 5. From the table, it shows that the performance of the turbine with addition of ODGV is higher than the performance of the base turbine without ODGV. The power coefficient of all ODGV modifications rises by 28 percent (with 8-blade ODGV) with Cp value of 0.1899, compared to the baseline turbine without ODGV that has Cp value of 0.1487. For 18-blade turbine

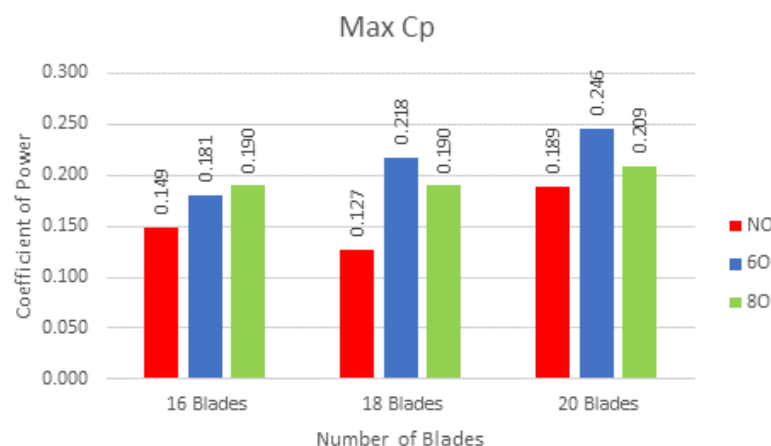


Figure 5. Power Coefficient of Turbine Configurations

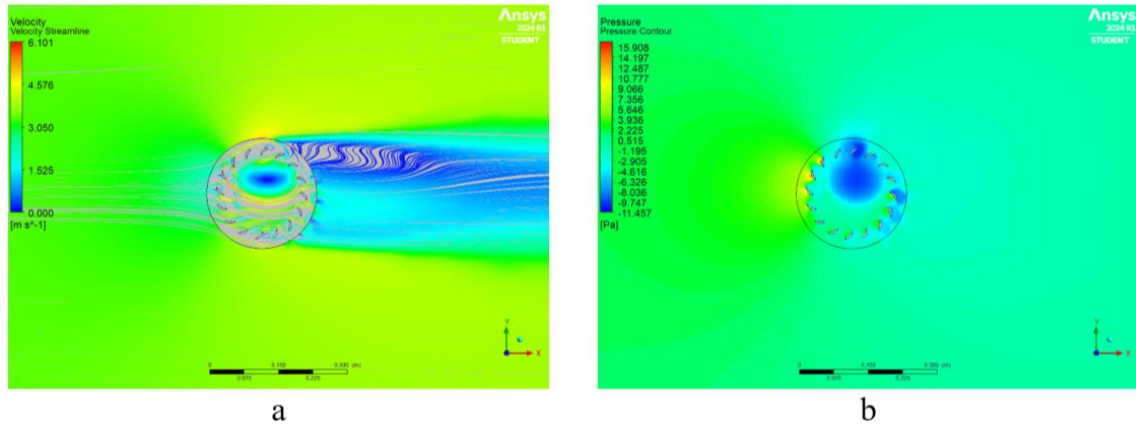


Figure 6. Distribution of velocity and pressure in the 16BNO configuration. (a) Velocity Streamline; (b) Pressure Contour.

configurations, the performance improvement with the addition of an ODGV is clearly illustrated in TABLE 4. From the table, it shows that the performance of the turbine with addition of ODGV is higher than the performance of the base turbine without ODGV. The power coefficient of all ODGV modifications rises by 71 percent (with 6-blade ODGV) with  $C_p$  value of 0.2176, compared with the baseline turbine without ODGV that has  $C_p$  value of 0.1273.

For 20-blade turbine configurations, the performance improvement with the addition of an ODGV is clearly illustrated in TABLE 3. From the table, it shows that the

performance of the turbine with addition of ODGV is higher than the performance of the base turbine without ODGV. The power coefficient of all ODGV modifications rises by 30 percent (with 6-blade ODGV) with  $C_p$  value of 0.2455, compared with the baseline turbine without ODGV that has  $C_p$  value of 0.1888.

Based on the improvement of the turbine, it is clear that the addition of an ODGV can significantly enhance the performance of wind turbine across various blade configurations. The performance improvements are evident in the increased power coefficients observed with the addition of ODGV compared to the base turbines.

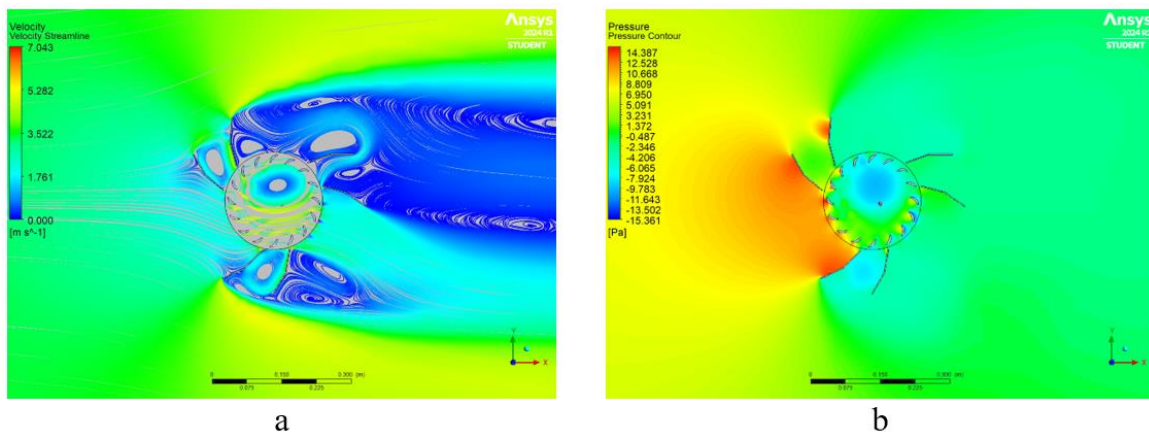


Figure 7. Distribution of velocity and pressure in the 16B6O configuration. (a) Velocity Streamline; (b) Pressure Contour.

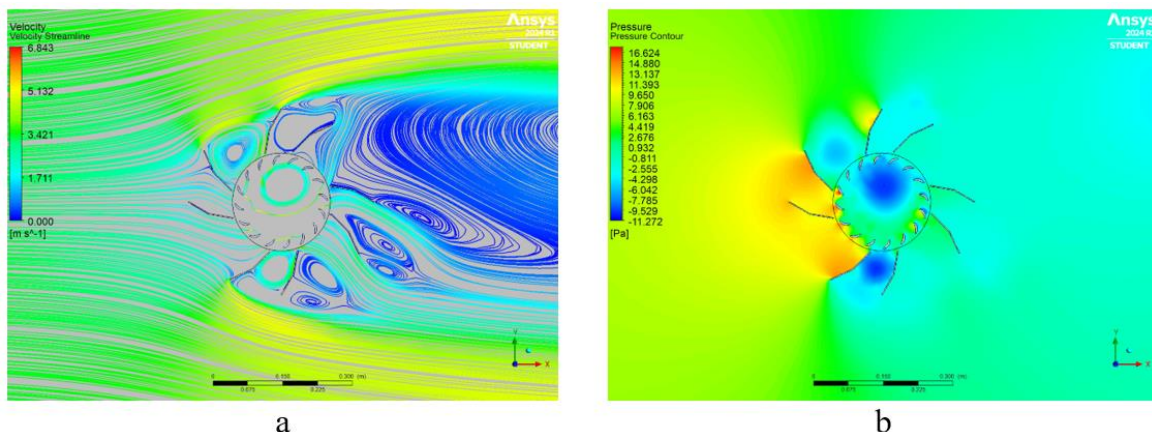


Figure 8. Distribution of velocity and pressure in the 16B8O configuration. (a) Velocity Streamline; (b) Pressure Contour.

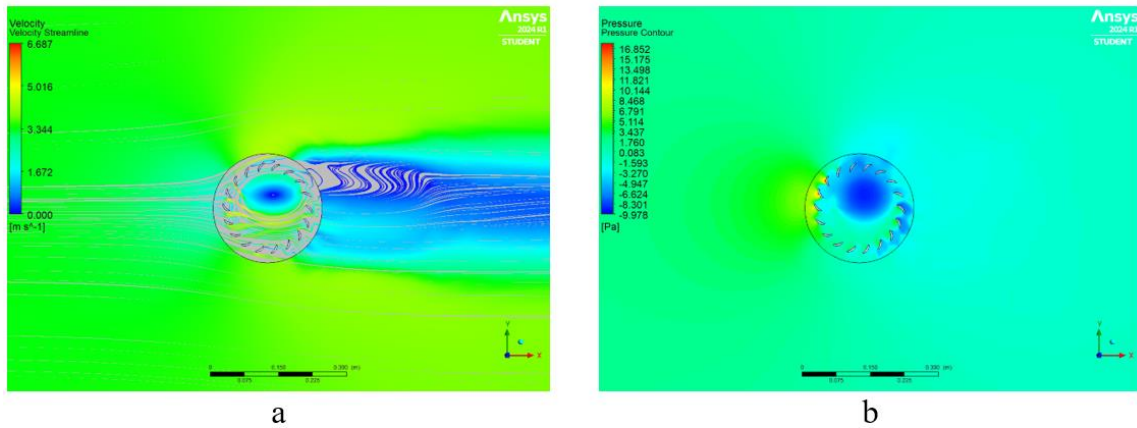


Figure 9. Distribution of velocity and pressure in the 18BNO configuration. (a) Velocity Streamline; (b) Pressure Contour.

These enhancements are consistent across different blade configurations, underscoring the effectiveness of ODGV in improving the overall performance of wind turbines. This makes ODGV a valuable component in the design and optimization of wind energy systems, particularly in maximizing energy capture and efficiency.

#### B. Numerical Flow Analysis of 16-blade Turbine

Flow simulations were performed on the turbine configuration. The simulation produces streamlines of fluid flow passing through the turbine and ODGV. For 16-blade turbine configurations, Figure 6 is the configuration without ODGV, and Figure 7 and Figure 8 for the

configuration with ODGV. Each configuration illustrate the differences in velocity streamlines. The addition of ODGV has an impact on the speed difference downstream of the rotor. In Figure 7a and Figure 8a, the velocity of the flow exiting the rotor is relatively greater than that of the flow in Figure 6a. The ODGV enhances the velocity of the downstream flow, as well as direct the wind flow more efficiently, reducing the impact on the returning side of the turbine. In addition, vortex phenomena were observed at several points on the ODGV.

The pressure distribution also varies notably with the addition of ODGV. In the baseline configuration (Figure 6b), the pressure on the upper and lower sides of the

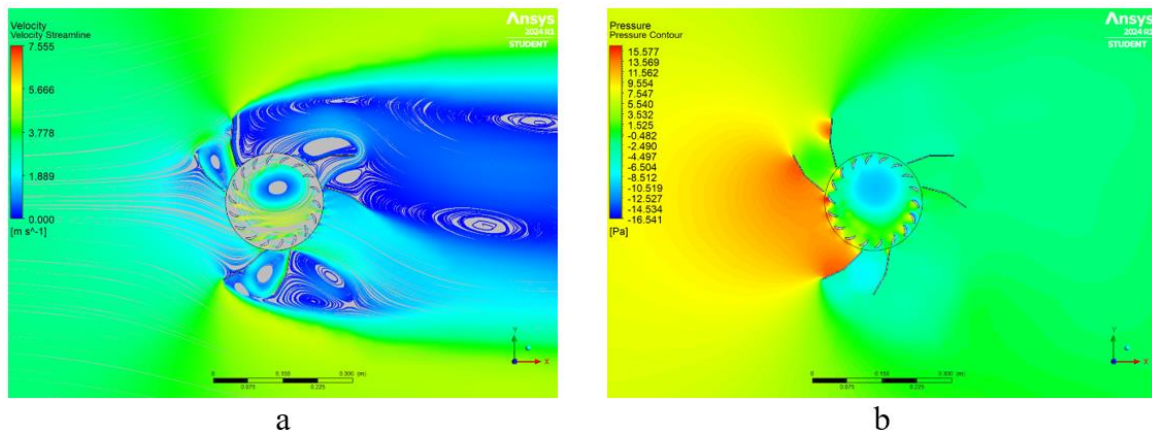


Figure 10. Distribution of velocity and pressure in the 18B6O configuration. (a) Velocity Streamline; (b) Pressure Contour.

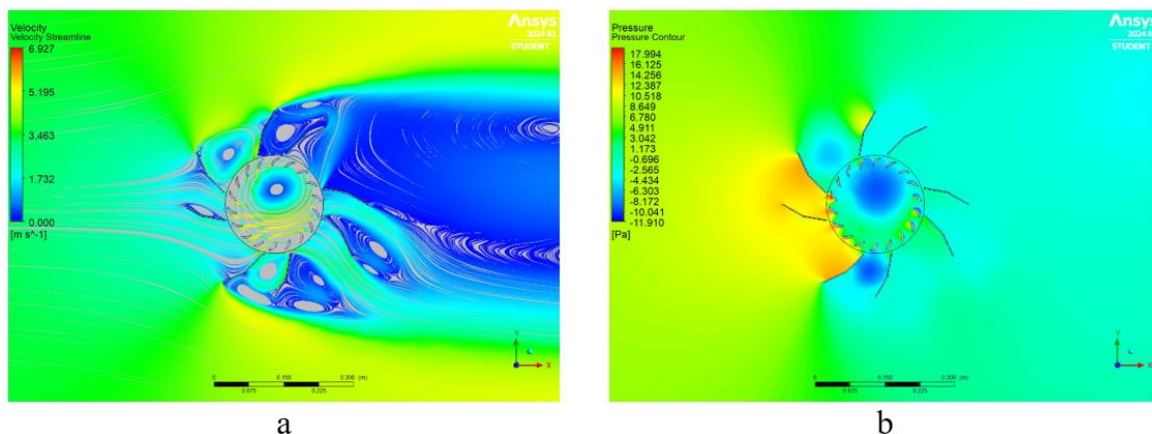


Figure 11. Distribution of velocity and pressure in the 18B8O configuration. (a) Velocity Streamline; (b) Pressure Contour.

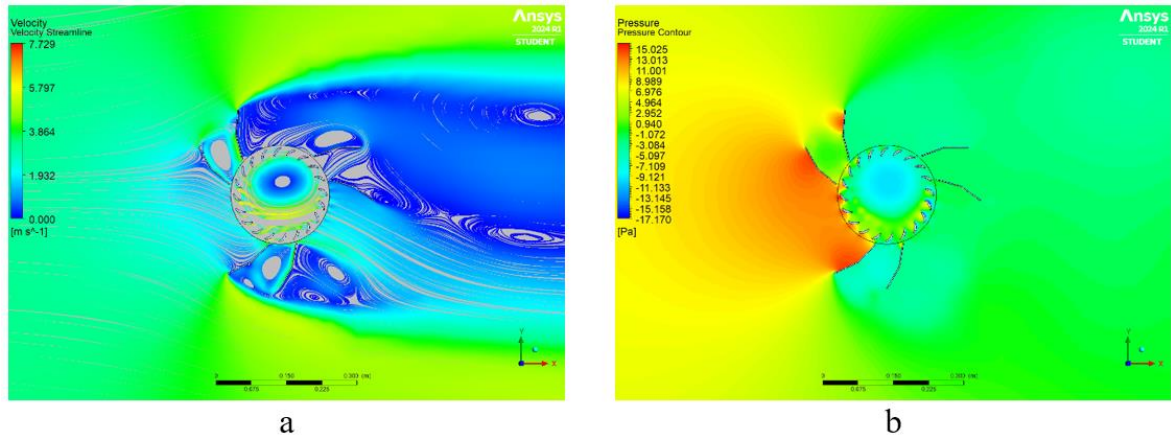


Figure 14. Distribution of velocity and pressure in the 20B6O configuration. (a) Velocity Streamline; (b) Pressure Contour.

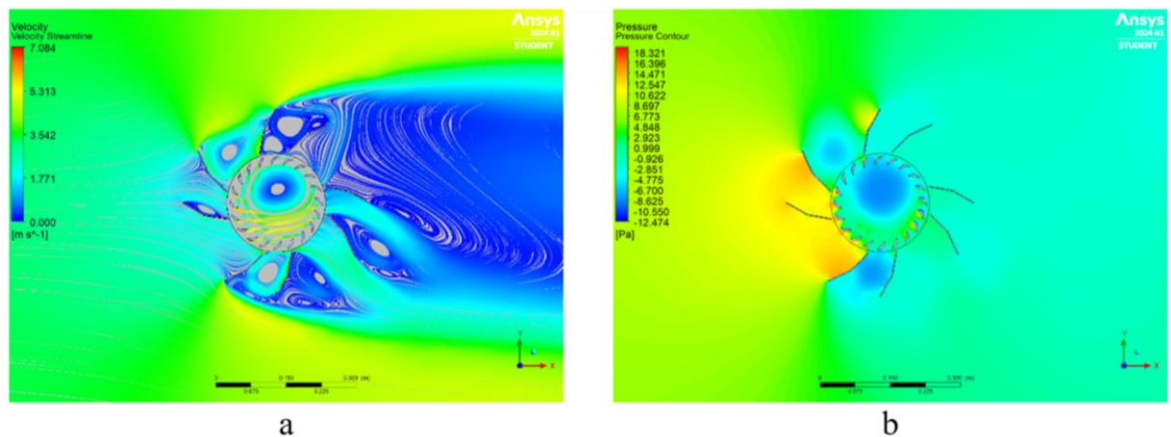


Figure 13. Distribution of velocity and pressure in the 20B8O configuration. (a) Velocity Streamline; (b) Pressure Contour.

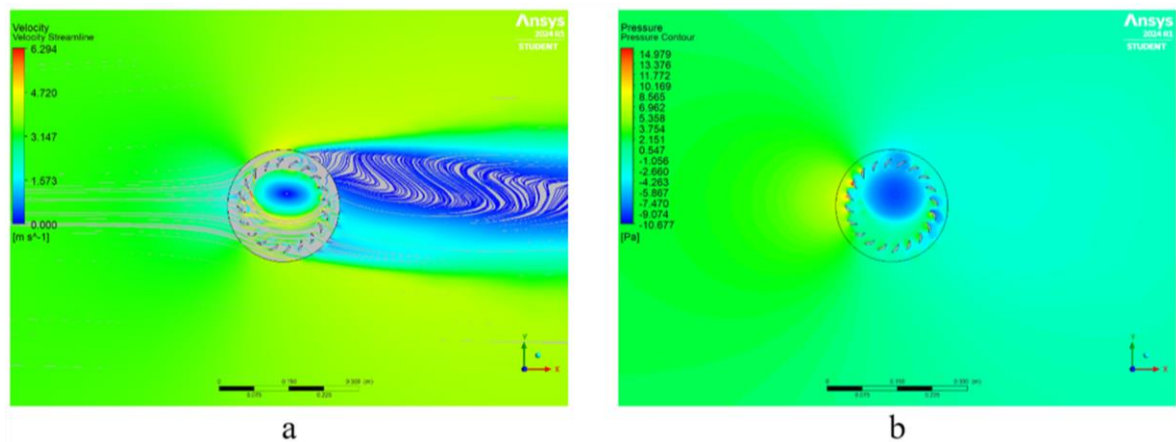


Figure 13. Distribution of velocity and pressure in the 20BNO configuration. (a) Velocity Streamline; (b) Pressure Contour.

turbine is balanced, resulting in less force to drive the turbine. Whereas in Figure 7b and Figure 8b where ODGV is applied, creates a significant pressure difference between the upper and the lower sides of the turbine, with the lower side experiencing higher pressure. This increased pressure on the upstream side provides additional force and energy to the turbine, thereby enhancing its rotational efficiency.

The amount of pressure is also influenced by the number of ODGV blades. In Figure 7b with 6 ODGV blades, there is more stable wind interaction, resulting in higher pressure due to concentrated wind flow. On the other hand, the turbine with 8 ODGVs (Figure 8b) shows a more divided wind flow with additional interactions,

leading to disturbances and slightly lower pressure between the ODGV blades.

In summary, the addition of ODGV improves the performance of the turbine by optimizing the flow velocity and increasing the pressure on the upstream side, thereby providing additional force and enhancing the energy output. The effectiveness of the ODGV is influenced by the number of blades, with different configurations producing varying levels of performance enhancement.

### C. Numerical Flow Analysis of 18-blade Turbine

For 18-blade turbine configurations, Figure 9 is the configuration without ODGV, and Figure 10 and Figure 11 for the configuration with ODGV. On base turbine without ODGV configuration, the 18-blade turbine captures more wind energy than the 16-blade turbine, leading to higher velocity. However, the introduction of ODGV (Figure 10a and Figure 11a) results in even higher velocity streams exiting the rotor. The ODGV directs the wind flow more efficiently, reducing the speed of wind hitting the turbine's upstream side while blocking the wind on the returning side, thus creating more directional flow.

The pressure distribution is also greatly influenced by the presence of ODGV. In Figure 9b, where the turbine is not applied with an ODGV, the pressure on the upper and lower sides of the turbine is balanced, making it difficult for the turbine to rotate efficiently. Whereas in Figure 10b and Figure 11b where ODGV is applied, there is a significant pressure difference between the upper and lower sides of the turbine where the lower side has a higher pressure. This pressure difference is critical for driving the turbine more effectively.

The number of ODGV blades affects the amount of pressure as well. In Figure 10b with 6 ODGV blades, the wind contact to the turbine is greater and a more stable wind flow, resulting in higher pressure. In the case with 8 ODGVs (Figure 11b), the wind flow is more divided and there is additional interaction with the ODGV blades which results in disturbance to the wind flow. This results in a smaller pressure between the ODGVs.

Overall, the addition of ODGV enhances the performance of the 18-blade turbine configurations by increasing the velocity and pressure, thereby providing more force and energy for efficient operation. This means ODGV can optimize the aerodynamic properties and overall performance of wind turbines.

### D. Numerical Flow Analysis of 20-blade Turbine

The flow simulations for the 20-blade turbine configurations, as depicted in Figure 13, Figure 14 and Figure 15, demonstrate some intriguing differences compared to the 16-blade and 18-blade setups. Unlike 18-blade turbine, the 20-blade base turbine configuration exhibits a lower velocity than the 18-blade base turbine, indicating a downside to having more blades due to increased turbine resistance. The increased solidity of the turbine with more blades leads to higher resistance, impacting the overall performance [25], [26].

With the addition of ODGV, significant improvements in velocity and pressure distribution are observed. In Figure 14a and Figure 15a shows that the velocity of the flow exiting the rotor is relatively greater than that of the flow in Figure 13a, where no ODGV is present. The ODGV effectively directs the wind flow, reducing the speed hitting the upstream side but blocking the returning side wind, resulting in a more streamlined flow.

Furthermore, the pressure distribution is profoundly influenced by the presence of ODGV. Without ODGV (Figure 13b), the pressure on the upper and lower sides of the turbine remains balanced, making it difficult for the

turbine to rotate efficiently. In contrast, with ODGV applied (Figure 14b and Figure 15b), there is a marked pressure difference between the upper and lower sides of the turbine, with the lower side experiencing higher pressure. This pressure differential is crucial for driving the turbine more effectively.

The number of ODGV blades also plays a significant role in determining the pressure dynamics. In Figure 14b with 6 ODGV blades, the wind contact with the turbine is greater due to the larger spacing between blades, resulting in a more stable wind flow and higher pressure. Conversely, the case with 8 ODGVs (Figure 15b) shows a more divided wind flow, with additional interaction causing disturbances and slightly lower pressure between the ODGV blades.

In summary, the addition of ODGV enhances the performance of the 20-blade turbine configurations by increasing the velocity and pressure, thereby providing more force and energy for efficient operation. This highlights the specific impact of ODGV on turbines with a higher number of blades, showcasing the balance between blade count and aerodynamics optimization.

## IV. Conclusion

Research has been conducted with the aim of finding the best configuration between wind turbines and ODGV. This research focus on the performance analysis of the turbine using Computational Fluid Dynamics method. Research data was obtained through numerical simulation with variation of blade counts and the addition of ODGV. Based on the results obtained, the addition of ODGV significantly enhances the performance of wind turbines across all configurations (16-blade, 18-blade, and 20-blade). The ODGV improves the aerodynamic efficiency by optimizing wind flow and creating a substantial pressure differential, resulting in higher power output.

The result shows that the 18-blade turbine configuration exhibits the highest improvement with ODGV, showing a remarkable 71 percent increase in power coefficient. The 20-blade configuration, despite having more blades, shows lower velocity in the baseline setup compared to the 18-blade turbine due to increase resistance. The ODGV still enhances performance but to a lesser degree than the 18-blade configuration.

In general, the highest performance is achieved by the 20-blade turbine and 6-blade ODGV configuration, with a value of power coefficient of 0.2455, which is 30 percent higher than the wind turbine without ODGV. These findings indicates that the addition of ODGV successfully plays a role in improving the performance of the cross-flow wind turbine.

## ACKNOWLEDGEMENTS

The author(s) would like to extend their gratitude to the Computing Laboratory of UPN Veteran Jakarta for providing the facilities for this research simulation.

## REFERENCES

- [1] A. Kalair, N. Abas, M. S. Saleem, A. R. Kalair, and N. Khan, "Role of energy storage systems in energy transition from fossil fuels to renewables," *Energy Storage*, vol. 3, no. 1, pp. 1–27, 2021, doi: 10.1002/est2.135.
- [2] T. Z. Ang, M. Saleem, M. Kamarol, H. S. Das, M. A. Nazari, and



- N. Prabakaran, "A comprehensive study of renewable energy sources: Classifications, challenges and suggestions," Sep. 01, 2022, *Elsevier Ltd.* doi: 10.1016/j.esr.2022.100939.
- [3] M. Kanoğlu, Y. A. Çengel, and J. M. Cimbala, *Fundamentals and Applications of Renewable Energy*, 1st ed. New York: Mc-Graw Hill Education, 2019.
- [4] W. Xu, Y. Li, G. Li, S. Li, C. Zhang, and F. Wang, "High-resolution numerical simulation of the performance of vertical axis wind turbines in urban area: Part II, array of vertical axis wind turbines between buildings," *Renew. Energy*, vol. 176, pp. 25–39, Oct. 2021, doi: 10.1016/j.renene.2021.05.011.
- [5] R. Kumar, K. Raahemifar, and A. S. Fung, "A critical review of vertical axis wind turbines for urban applications," Jun. 01, 2018, *Elsevier Ltd.* doi: 10.1016/j.rser.2018.03.033.
- [6] N. Alom and U. K. Saha, "Evolution and progress in the development of savonius wind turbine rotor blade profiles and shapes," Jun. 01, 2019, *American Society of Mechanical Engineers (ASME)*. doi: 10.1115/1.4041848.
- [7] I. C. Mandiş, D. N. Robescu, and M. Bărglăzan, "Capitalization of wind potential using a modified Banki turbine," *UPB Sci. Bull. Ser. D Mech. Eng.*, vol. 70, no. 4, pp. 115–124, 2008.
- [8] D. M. Kurniawati, D. D. P. Tjahjana, and B. Santoso, "Experimental investigation on performance of crossflow wind turbine as effect of blades number," in *AIP Conference Proceedings*, American Institute of Physics Inc., Feb. 2018. doi: 10.1063/1.5024104.
- [9] S. Susanto, D. D. P. Tjahjana, and B. Santoso, "Experimental tests of the effect of rotor diameter ratio and blade number to the cross-flow wind turbine performance," in *AIP Conference Proceedings*, American Institute of Physics Inc., Feb. 2018. doi: 10.1063/1.5024101.
- [10] A. Hidayat and A. I. Ismail, "Simulation of Wind Turbines with Variation of Number of Blades and Blades Angle on Turbine Performance," no. Iconit 2019, pp. 115–118, 2020, doi: 10.5220/0009423101150118.
- [11] R. Iliev, "Experimental analysis of cross-flow wind turbine with omni-directional multi-nozzle," in *IOP Conference Series: Earth and Environmental Science*, Institute of Physics, 2023. doi: 10.1088/1755-1315/1128/1/012012.
- [12] A. Wibowo, D. D. P. Tjahjana, B. Santoso, and M. R. C. Situmorang, "Study of turbine and guide vanes integration to enhance the performance of cross flow vertical axis wind turbine," in *AIP Conference Proceedings*, American Institute of Physics Inc., Feb. 2018. doi: 10.1063/1.5024102.
- [13] Y. A. Wicaksono, D. D. P. Tjahjana, and S. Hadi, "Influence of omni-directional guide vane on the performance of cross-flow rotor for urban wind energy," in *AIP Conference Proceedings*, American Institute of Physics Inc., Feb. 2018. doi: 10.1063/1.5024099.
- [14] Z. Sefidgar, A. Ahmadi Joneidi, and A. Arabkoohsar, "A Comprehensive Review on Development and Applications of Cross-Flow Wind Turbines," *Sustain.*, vol. 15, no. 5, 2023, doi: 10.3390/su15054679.
- [15] W. T. Chong, A. Fazlizan, S. C. Poh, K. C. Pan, W. P. Hew, and F. B. Hsiao, "The design, simulation and testing of an urban vertical axis wind turbine with the omni-direction-guide-vane," *Appl. Energy*, vol. 112, pp. 601–609, 2013, doi: 10.1016/j.apenergy.2012.12.064.
- [16] W. Yahya *et al.*, "Study the influence of using guide vanes blades on the performance of cross-flow wind turbine," *Appl. Nanosci.*, vol. 13, no. 2, pp. 1115–1124, Feb. 2023, doi: 10.1007/s13204-021-01918-0.
- [17] V. Obretenov and R. Iliev, "Investigations of a vertical axis wind turbine with frontal cylindrical guide vane unit," *E3S Web Conf.*, vol. 327, 2021, doi: 10.1051/e3sconf/202132704005.
- [18] K. Kołodziejczyk and R. Ptak, "Numerical Investigations of the Vertical Axis Wind Turbine with Guide Vane," *Energies*, vol. 15, no. 22, 2022, doi: 10.3390/en15228704.
- [19] T. Tanino, R. Yoshihara, and T. Miyaguni, "A Study on a Casing Consisting of Three Flow Deflectors for Performance Improvement of Cross-Flow Wind Turbine," *Energies*, vol. 15, no. 16, Aug. 2022, doi: 10.3390/en15166093.
- [20] K. H. Wong *et al.*, "The design and flow simulation of a power-augmented shroud for urban wind turbine system," in *Energy Procedia*, Elsevier Ltd, 2014, pp. 1275–1278. doi: 10.1016/j.egypro.2014.11.1080.
- [21] I. Sadreghighi, "Mesh Sensitivity & Mesh Independence Study CFD Open Series," 2021. doi: 10.13140/RG.2.2.34847.51365/2.
- [22] H. K. Versteeg and W. Malalasekera, *An Introduction to Computational Fluid Dynamics Second Edition*, Second Ed. Harlow: Pearson Education Limited, 2007. [Online]. Available: [www.pearsoned.co.uk/versteeg](http://www.pearsoned.co.uk/versteeg)
- [23] S. Younoussi and A. Ettaouil, "Calibration method of the k- $\omega$  SST turbulence model for wind turbine performance prediction near stall condition," *Heliyon*, vol. 10, no. 1, p. e24048, 2024, doi: <https://doi.org/10.1016/j.heliyon.2024.e24048>.
- [24] Z. Xu, X. Dong, K. Li, Q. Zhou, and Y. Zhao, "Study of the Self-starting Performance of a Vertical-axis Wind Turbine," *J. Appl. Fluid Mech.*, vol. 17, no. 6, pp. 1261–1276, 2024, doi: 10.47176/jafm.17.6.2295.
- [25] T. TANINO and S. NAKAO, "Influence of Number of Blade and Blade Setting Angle on the Performance of a Cross-flow Wind Turbine," *Trans. Japan Soc. Mech. Eng. Ser. B*, vol. 73, pp. 225–230, 2007, doi: 10.1299/kikaib.73.225.
- [26] Q. Clémentot, P.-L. Delafin, and T. Maître, "Numerical study of an innovative cross-flow turbine," in *17èmes Journées de l'Hydrodynamique*, Cherbourg-en-Cotentin (web conference), France, Nov. 2020. [Online]. Available: <https://hal.science/hal-03120167>